FINAL REPORT

EFFICIENT NONLINEAR CONVERSION OF LASER DIODE PUMPED MINIATURE SOLID STATE LASER SOURCES

CONTRACT NUMBER: DAAL03-86-C0007

Submitted to:

U.S. Army Research Office
P.O. Box 12211
Research Triangle Park, North Carolina 27709

by:

David C. Gerstenberger and Richard W. Wallace

LIGHTWAVE Electronics Corporation
1161 San Antonio Road
Mountain View, California 94043

June 1989

MASTER COPY - FOR REPRODUCTION PURPOSES

UNCLASSIFIED
SECURITY CLASSIFICATION OF THIS PAGE (When Data Entered)

REPORT DOCUMENTATION PAGE		READ INSTRUCTIONS BEFORE COMPLETING FORM
1. REPORT NUMBER ARO 23290.2-PH-S	2. GOVT ACCESSION NO. N/A	3. RECIPIENT'S CATALOG NUMBER N/A
4. TITLE (and Subtitle) EFFICIENT NONLINEAR CONVERSION OF LASER DIODE PUMPED MINIATURE SOLID STATE LASER SOURCES		5. TYPE OF REPORT & PERIOD COVERED FINAL REPORT 1 MAY 1986-30 APRIL 1989 6. PERFORMING ORG. REPORT NUMBER
7. AUTHOR(s) DAVID C. GERSTENBERGER AND RICHARD W. WALLACE		8. CONTRACT OR GRANT NUMBER(s) DAAL03-86-C0007
9. PERFORMING ORGANIZATION NAME AND ADDRESS Lightwave Electronics Corporation 1161 San Antonio Road Mountain View, CA. 94043		10. PROGRAM ELEMENT, PROJECT, TASK AREA & WORK UNIT NUMBERS
11. CONTROLLING OFFICE NAME AND ADDRESS U. S. Army Research Office Post Office Box 12211 Research Triangle Park, NC 27709		12. REPORT DATE June, 1989 13. NUMBER OF PAGES
14. MONITORING AGENCY NAME & ADDRESS(if different from Controlling Office)		15. SECURITY CLASS. (of this report) Unclassified 15a. DECLASSIFICATION/DOWNGRADING SCHEDULE

16. DISTRIBUTION STATEMENT (of this Report)

Approved for public release; distribution unlimited.

17. DISTRIBUTION STATEMENT (of the abstract entered in Block 20, if different from Report)

NA

18. SUPPLEMENTARY NOTES

The view, opinions, and/or findings contained in this report are those of the author(s) and should not be construed as an official Department of the Army position, policy, or decision, unless so designated by other documentation.

19. KEY WORDS (Continue on reverse side if necessary and identify by block number)

NONLINEAR CONVERSION, DIODE PUMPED SOLID STATE LASER

20. ABSTRACT (Continue on reverse side if necessary and identify by block number)

THIS RESEARCH PROGRAM HAS DEALT WITH THE DEVELOPMENT OF EFFICIENT AND COMPACT SOURCES OF VISIBLE LASER LIGHT BASED ON THE NONLINEAR OPTICAL CONVERSION OF THE OUTPUTS OF DIODE PUMPED SOLID STATE LASERS. INTRACAVITY FREQUENCY DOUBLING, FREQUENCY DOUBLING OF CONTINUOUS WAVE SINGLE FREQUENCY NONPLANAR RING Nd: YAG LASERS IN EXTERNAL RESONANT CAVITIES AND SINGLE PASS DOUBLING OF DIODE PUMPED Q-SWITCHED LASERS WERE STUDIED. NONLINEAR MATERIALS INCLUDING LITHIUM DIFFUSED LITHIUM NIOBATE, MAGNESIUM OXIDE DOPED LITHIUM NIOBATE AND POTASSIUM

DD FORM 1 JAN 73 1473 EDITION OF 1 NOV 65 IS OBSOLETE

UNCLASSIFIED
SECURITY CLASSIFICATION OF THIS PAGE (When Data Entered)

BLOCK 20 CONTINUED

TITANYL PHOSPHATE WERE EXAMINED.

WE OBTAINED 45mW OF cw GREEN LIGHT AN MONOLITHIC EXTERNALLY RESONANT CAVITY CONSTRUCTED OF MgO:$LiNbO^3$ PUMPED BY A 200mW SINGLE FREQUENCY Nd:YAG LASER. THIS DOUBLER WAS ELECTRO-OPTICALLY LOCKED INTO RESONANCE WITH THE LASER OSCILLATOR AND MAINTAINED AT PHASEMATCHING TEMPERATURE BY A MINIATURE PLATINUM HYBRID HEATER-SENSOR ELEMENT AND CONTROL CIRCUIT. PEAK POWER OVER 200mW IN THE GREEN WERE MEASURED WITH THIS DOUBLING DEVICE WHEN PUMPED BY A SINGLE FREQUENCY PULSED 500mW SOURCE.

WE ALSO OBSERVED SECOND HARMONIC ENERGY CONVERSION EFFICIENCIES AS HIGH AS 50% USING DIODE PUMPED Q-SWITCHED LASER SOURCES.

FINAL REPORT

EFFICIENT NONLINEAR CONVERSION OF LASER DIODE PUMPED MINIATURE SOLID STATE LASER SOURCES

ABSTRACT

This research program has dealt with the development of efficient and compact sources of visible laser light based on the nonlinear optical conversion of the outputs of diode pumped solid state lasers. Intracavity frequency doubling, frequency doubling of continuous wave single frequency nonplanar ring Nd:YAG lasers in external resonant cavities and single pass doubling of diode pumped Q-switched lasers were studied. Nonlinear materials including lithium diffused lithium niobate, magnesium oxide doped lithium niobate and potassium titanyl phosphate were examined.

We obtained 45 mW of cw green light from an monolithic externally resonant cavity constructed of $MgO:LiNbO_3$ pumped by a 200 mW single frequency Nd:YAG laser. This doubler was electro-optically locked into resonance with the laser oscillator and maintained at phasematching temperature by a miniature platinum hybrid heater-sensor element and control circuit. Peak powers over 200 mW in the green were measured with this doubling device when pumped by a single frequency pulsed 500 mW source.

We also observed second harmonic energy conversion efficiencies as high as 50% using diode pumped Q-switched laser sources.

TABLE OF CONTENTS

EFFICIENT NONLINEAR CONVERSION OF LASER DIODE PUMPED MINIATURE SOLID STATE LASER SOURCES

INTRODUCTION

Solid state lasers pumped by laser diodes have been studied for over 20 years. Recent progress has lead to commercially available ultra-stable single frequency continuous wave lasers and kilowatt peak power pulsed lasers with optical efficiencies greater than 20% [1,2]. The use of diode lasers with electrical to optical efficiency of nearly 50% [3] to pump solid state lasers can provide laser devices with overall efficiency of nearly 10% in the infrared. In this research program, we have concentrated on perfecting nonlinear optical techniques to efficiently convert the output of these infrared lasers to the visible spectral region.

We used two diode pumped laser products developed at LIGHTWAVE Electronics as sources for our nonlinear optical experiments. The first of these devices is a cw single frequency Nd:YAG laser invented by Kane and Byer [4] at Stanford University and developed into commercial products at LIGHTWAVE Electronics. This laser is shown in Figure 1 and utilizes a monolithic non-planar ring geometry (MISER) for the Nd:YAG laser cavity to provide powerful, stable and efficient output at 1064nm. We used the technique of resonant enhancement in an external optical cavity [5,6] to efficiently frequency double the cw 1064nm laser.

The second diode pumped product developed at LIGHTWAVE Electronics is a Q-switched solid state laser. These devices are capable of kilowatt power level pulses, so that more conventional single pass frequency doubling geometries could be employed.

The initial developments of both of these lasers was done under this contract. From these developments, we obtained SBIR funding to commercialize these products. There are now over 350 ring lasers in the field. The Q-switched lasers are being delivered at a rate of two per week.

In the next section we will summarize the theory of harmonic conversion in an external resonant cavity and our experiments and results with cw lasers. The following section describes pulsed laser results. Finally, conclusions and recommendations are presented in the last section.

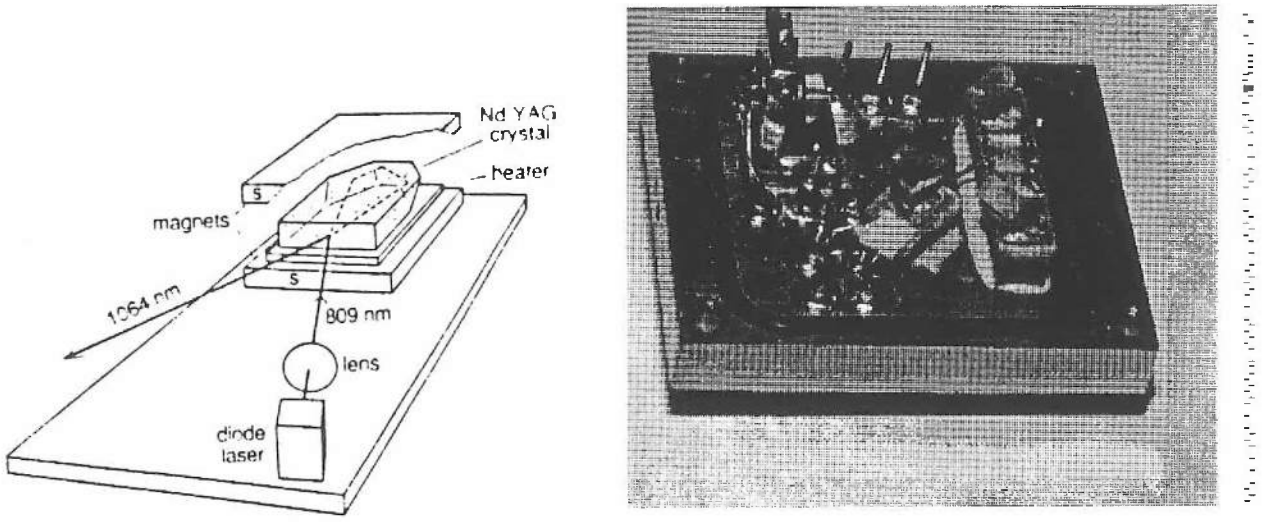

Figure 1: Diode Laser Pumped Non-planar Ring Nd:YAG Laser. The drawing on the left is a schematic representation of the cw single frequency 1064nm laser invented by Kane and Byer [4]. The photograph on the right shows the commercial version developed at LIGHTWAVE Electronics. The laser shown is a 40 mW Model 120-03. The laser uses a 160 mW diode pump laser and is approximately 2"x2"x1" tall.

FREQUENCY DOUBLING IN AN EXTERNAL RESONANT CAVITY

THEORY

The efficiency of frequency conversion from the fundamental wave to the second harmonic in a nonlinear medium is given by [7],

$$\frac{P_2}{P_1} = \mathrm{TANH}^2\left[1 \sqrt{K\frac{P_1}{A}}\ \frac{\sin \Delta kl/2}{\Delta kl/2} \right] \qquad (1)$$

where P_1 and P_2 are the fundamental and second harmonic powers, l is the length of the nonlinear crystal, A is the area of the fundamental beam and Δkl is the phase mismatch between the second harmonic polarization wave driven by the fundamental beam and the second harmonic electro-magnetic wave. The coefficient K is,

$$K = 2(377/n)^3 w_1^2 d_{eff}^2 \qquad (2)$$

where n is the refractive index, w_1 is the optical frequency of the fundamental beam and d_{eff} is the effective nonlinear coefficient of the nonlinear crystal.

For low conversion efficiencies, Equation (1) can be simplified to,

$$\frac{P_2}{P_1} = l^2 K \frac{P_1}{A} \mathrm{sinc}^2(\Delta kl/2) = g_{SH}. \qquad (3)$$

Clearly, the highest conversion efficiency occurs for Δkl equal zero which is the phase-matched condition. In that case, Equation (3) can be further simplified to,

$$P_2 = l^2 P_1^2 K/A. \qquad (4)$$

Thus, in the low conversion limit, second harmonic power varies as the square of the fundamental. For relatively

low powered cw lasers such as diode pumped Nd:YAG devices, the conversion is typically quite low. In the case of a lithium niobate crystal 10mm long with optimum focussing, the nonlinear conversion coefficient is approximately .004 per Watt of fundamental power which corresponds to a second harmonic power of 10 microwatts for an incident fundamental power of 50 milliwatts. For a fundamental power of 250 mW, 0.25 mW of second harmonic would be produced.

One way around the problem of low conversion efficiency for cw lasers is to place the nonlinear crystal inside the laser cavity to exploit the high intracavity circulating power [8]. In a preliminary experiment, we obtained 48 mW of cw 532nm light from a diode pumped linear cavity Nd:YAG laser using an intracavity KTP crystal. The same laser provided 240 mW at 1064nm when optimized for operation without the KTP. The green light produced by intracavity doubling with KTP had nearly 100% amplitude modulation. Noise of this magnitude on the green beam makes it useless for most applications. Other researchers have observed similar modulation of the output of diode pumped lasers intracavity doubled with KTP [9].

We also repeated the experiments of Oka and Kubota [10] who used an intracavity quarter wave plate to stabilize the green output of an intracavity frequency doubled diode pumped Nd:YAG laser. We were unable to duplicate their "quiet" results.

An alternative approach for low power lasers which is especially attractive using the single frequency nonplanar ring laser source is the technique of resonant enhancement in an external optical cavity. Theory and experiments in this area were conducted initially by Ashkin and co-workers [5] and more recently by Kozlovsky et al [6]. The enhancement in an external resonant ring cavity such as the one shown schematically in Figure 2 is given by,

$$P_C/P_1 = T_1/(1 - \sqrt{R_1 R_m})^2 \qquad (5)$$

where P_C is the circulating power in the resonant cavity, P_1 is the incident 1064nm power, T_1 is the power transmission coefficient of the input mirror and R_1 is the power reflection coefficient of the input mirror. For a lossless mirror, $R_1 + T_1 = 1$. R_m is related to losses in the external cavity by,

$$R_m = T_o(1 - g_{SH}P_C)R_2 \qquad (6)$$

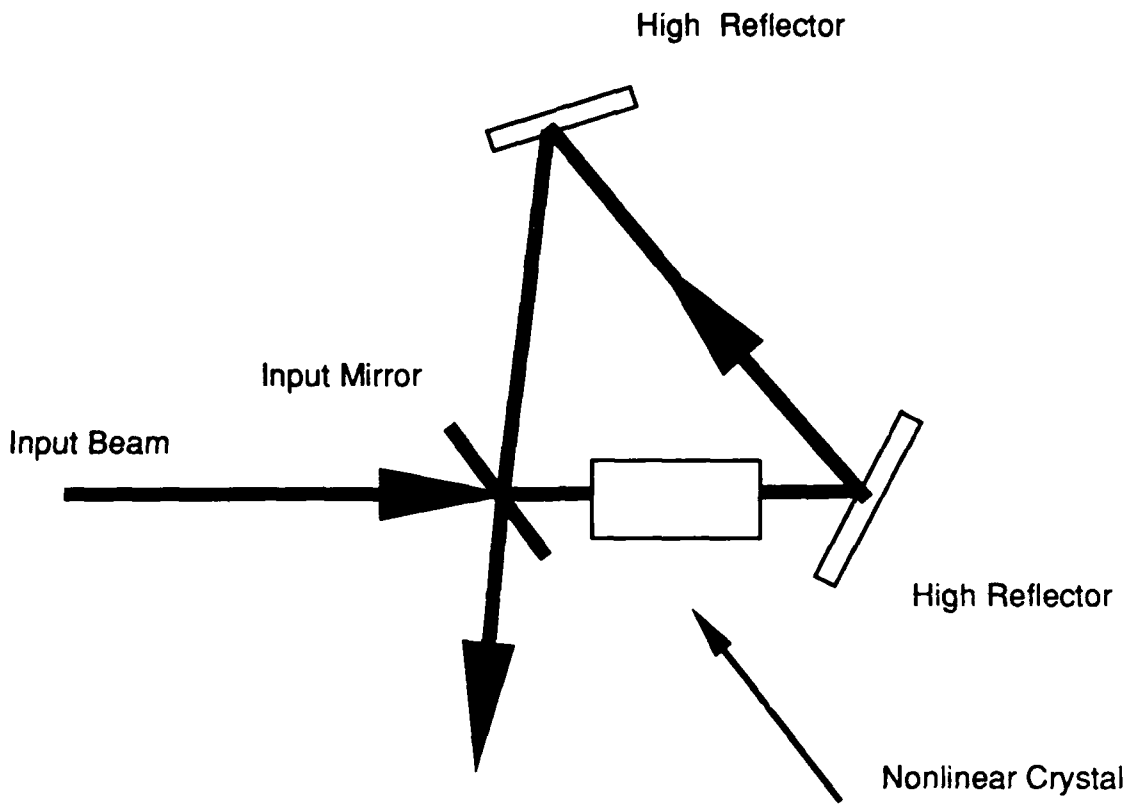

Figure 2: Resonant Ring Cavity for External Harmonic Generation. This three mirror cavity consists of two high reflector mirrors and one "input" mirror. When the cavity is resonant with the frequency of the input beam, a large optical field builds up, limited by the finesse of the cavity. The transmission of the input mirror is selected to match the other losses in the cavity, including scatter and absorption in the other mirrors and the nonlinear crystal, transmission through the high reflector mirrors and conversion to the second harmonic in the nonlinear crystal.

where T_o is the power transmission of one round trip through the bulk of the nonlinear crystal and R_2 is the product of the power reflection coefficients of the remaining mirrors in the ring cavity. Finally, the generated second harmonic power is,

$$P_c = g_{SH} P_c^2. \qquad (7)$$

Maximum circulating power and hence second harmonic power are produced when the output mirror reflectivity R_1 is made equal to R_m. In that "impedance matched" case [6],

$$P_c = P_1/(1 - R_1). \qquad (8)$$

Second harmonic power as a function of intracavity loss calculated from the above model is shown in Figure 3 for an assumed 50 mW of incident 1064nm power. Nonlinear conversion coefficients of .001, .002, .005 and .010 per Watt are assumed. As mentioned above, a value of .004 per Watt is calculated for lithium niobate with confocal focussing in a 10mm long crystal. Larger values are appropriate for materials with larger nonlinear coefficients, d_{eff}, such as barium sodium niobate. Smaller values are appropriate for weaker focussing, for materials with smaller nonlinear coefficients or for crystals with shorter phase matchable lengths. As is clearly seen in Figure 3, the second harmonic power is a strong function of intracavity loss. Good conversion efficiency can only be obtained when intracavity losses are low.

In Figure 4, the variation of second harmonic power versus input mirror power transmission coefficient is displayed. Part A shows power variation for an assumed incident power of 50 mW and intracavity loss of 0.5%. Part B shows power variation for an assumed loss of 2.0%. Both graphs show calculated powers for both .001 and .010 per Watt nonlinear conversion coefficients. We used these curves, which bracket the parameter space in which we expect to operate, to determine the value of mirror transmission to use in our external resonant cavity experiments. We chose $1.5 \pm 0.5\%$ transmitting mirrors.

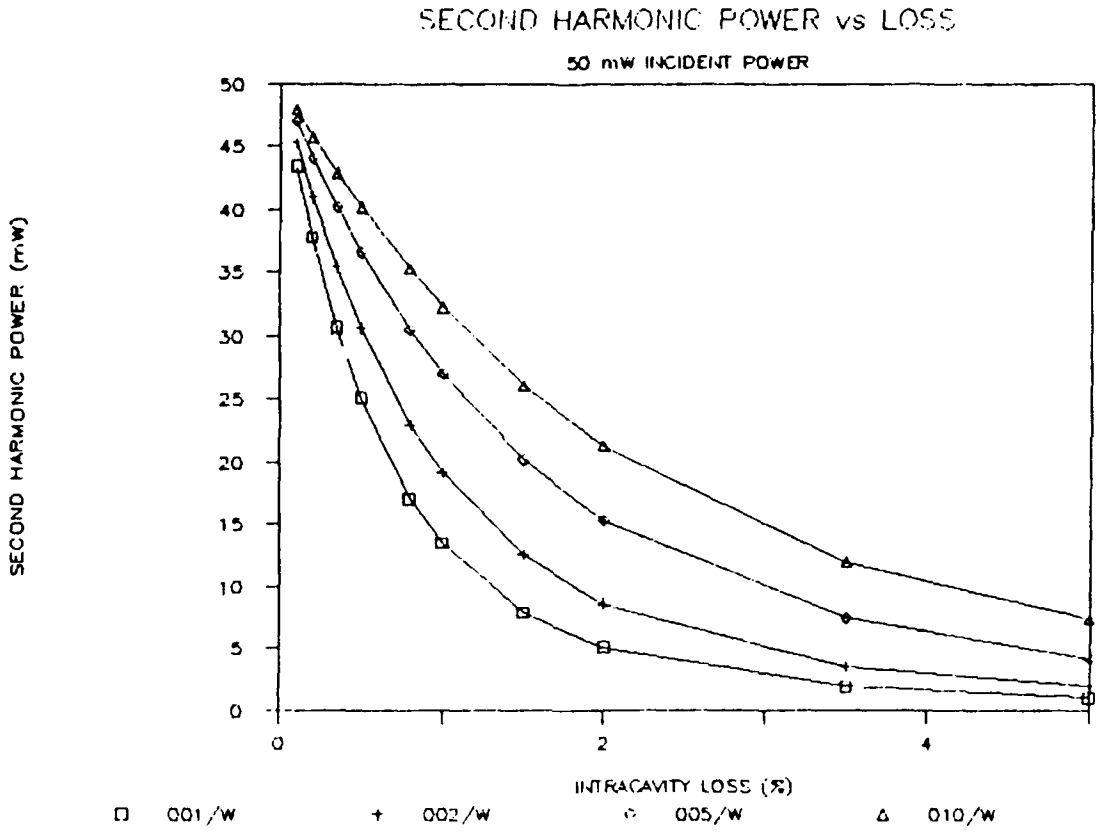

Figure 3: Second Harmonic Power versus Intracavity Loss. The effect of intracavity loss on second harmonic power is shown for several values of nonlinear conversion coefficient. An incident fundamental power of 50 mW is assumed. The low conversion efficiency limit is also assumed, which is only valid for second harmonic powers less than about 25 mW.

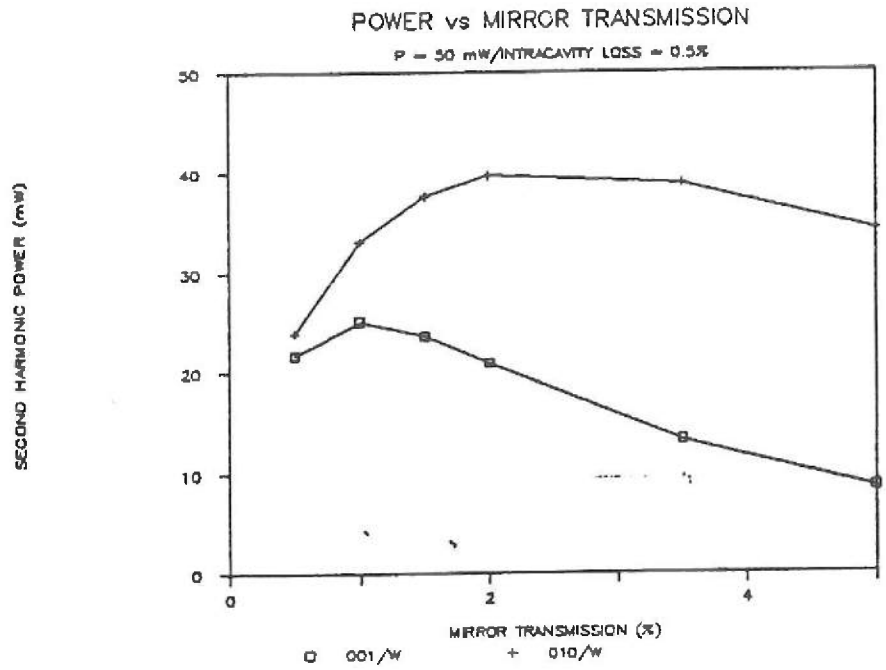

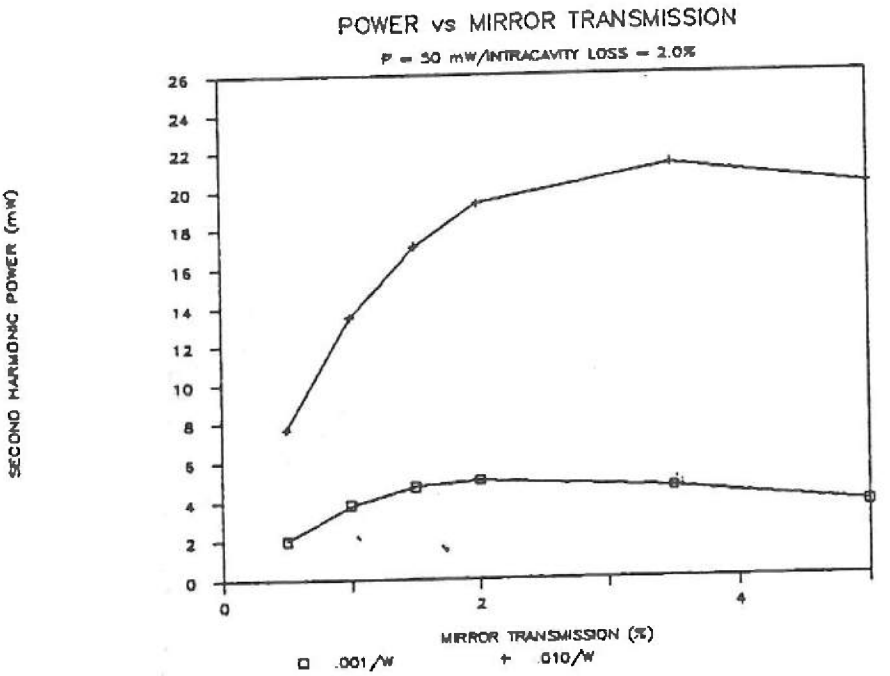

Figure 4: Second Harmonic Power versus Input Mirror Transmission. Incident fundamental power is assumed to be 50 mW. For (A), intracavity loss = 0.5%; for (B), loss = 2.0%. Curves are shown for g_{SH} = .001/W and .010/W.

EXPERIMENTS

Monolithic MgO:$LiNbO_3$ Resonant Doublers

Our initial experiments were conducted with magnesium oxide doped lithium niobate crystals. This material can be 90° phasematched for frequency doubling 1064nm light by temperature tuning near 107°C [11]. Secondly, crystals with axial uniformity sufficient to phasematch over lengths up to 25mm could be grown [11]. Finally, the magnesium oxide doping had been shown to significantly improve the resistance of lithium niobate to photorefractive damage [12].

Our first crystal resonator devices employed a geometry shown in Figure 5. This design is similar to a design used by Kozlovsky [6]. The crystals were approximately 12mm long with 7mm radius of curvature mirrors at either end. One curved surface was coated as a high reflector for 1064nm and a high transmitter for 532nm. The other curved surface was the input mirror and was coated to have approximately 98.5% reflectivity at 1064nm. One side of the crystal was polished and not coated and served as a total internal reflecting surface. The resonator was designed so that both linear and ring modes were contained within the crystal.

Light from a 50mW single frequency laser was coupled through a Faraday isolator and mode matched into the linear resonator mode of the crystal. Approximately 25mW of 1064nm light was incident on the crystal. We obtained a total of 3.1mW of 532nm light from the resonant doubler, approximately 50% from each end.

The crystal was maintained at phasematching temperature using a pair of platinum thin film resistors intertwined on an alumina substrate. One of the resistors served as a temperature probe and the other as a heating element. The probe resistor was electrically connected to one leg of a bridge circuit which supplied a correction signal to control power supplied to the heater resistor. The doubler crystal and resistor pair were close-coupled with an aluminum crystal holder and the combination inserted in a glass vacuum bottle to insulate them from the surrounding atmosphere, provide for uniform temperature over the length of the crystal and minimize the heat required to maintain the crystal at phasematching temperature. A photograph of the platinum element, doubler crystal and vacuum bottle is shown in Figure 6.

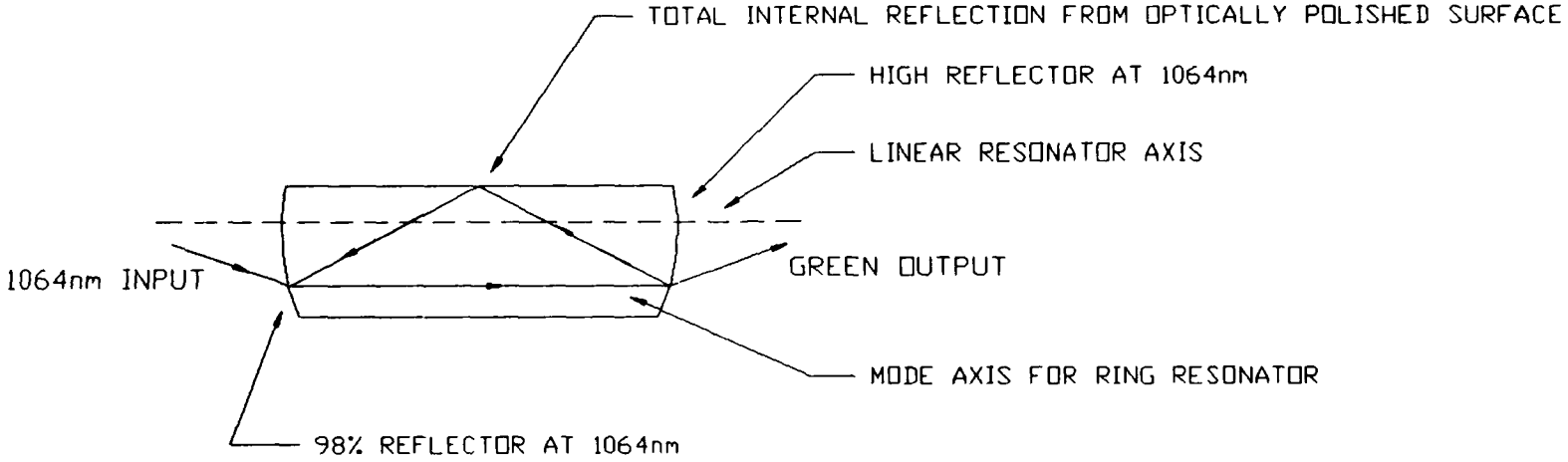

FIGURE 5: Monolithic Resonant Optical Converter. The high Q optical cavity defined by the 98% and high reflecting coatings on the ends of the crystal can lead to large enhancements of the 1064nm light inserted through the 98% reflecting 'input' coating. An electric field is applied across the crystal perpendicular to the plane of this drawing. The field electro-optically tunes the resonator to resonance with the incident single frequency light. The crystal can be operated either as a linear cavity or a ring cavity by proper positioning and orientation of the crystal relative to the input beam. Two advantages of the ring mode of operation are elimination of backreflected 1064nm light to the source laser and the fact that a single leg of the ring mode parallel to the linear axis can be phase-matched, so that the second harmonic will leak out one end, as shown. Dimensions of the lithium niobate crystal shown above are 11mm long by 4mm wide by 2mm thick.

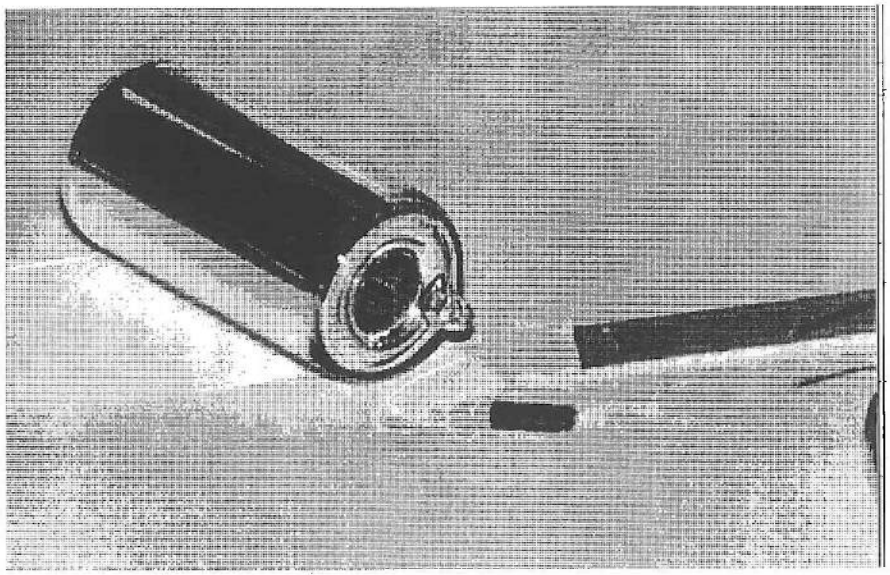

Figure 6: Linear Doubler Crystal, Platinum Heater-Sensor Element and Vacuum Bottle. The 12mm long doubler crystal was mounted on an aluminum holder (not shown) and topped with the 50mm long 8mm wide platinum heater-sensor element. This combination was inserted into the center hole of the pyrex vacuum bottle. Approximately 500 mW of heat was required to maintain the crystal at the 110^{o}C phasematching temperature.

In order to measure intercavity loss and gain a better understanding of the limitations of second harmonic generation in our resonant doubler, we attempted to measure the finesse of the MgO:$LiNbO_3$ resonant cavity by slowly scanning the frequency of the 1064nm light and detecting the 1064nm light that was transmitted through the crystal. We observed significant assymmetry in the width and shape of transmission peaks of the doubler crystal. Representative traces are shown in Figure 7. The free spectral range of the cavity is 5.7GHz. The expected finesse for a lossless Fabry-Perot interferometer with one high reflector and one 98.5% reflector is 417. The full width at half maximum for transmission peaks is then expected to be 13.7MHz. As can be seen in Figure 7, the full width at half maximum depends on the direction in which the frequency of the 1064nm light is scanned.

The assymmetry can be understood as follows. The power at 1064nm builds up inside the doubler crystal cavity as the frequency approaches a cavity resonance. Intracavity absorption of the 1064nm light heats the crystal locally and shifts the resonant frequency at a rate that we independently measured to be about -4.4GHz per degree Centigrade. In one direction, the shift of the cavity resonance and the scanning 1064nm frequency are in the same direction and the transmission peak is broadened. In the other direction, the scan frequency and thermally induced frequency shift are opposite and the transmission peak is narrowed. Examples of both of these cases are shown in Figure 7. Intracavity absorption of the magnitude implied by these results is a big problem as it limits the conversion efficiency to the second harmonic. We estimate the total intracavity loss to be on the order of 2%.

Due to fabrication problems, we were unable to operate the crystal in the ring configuration because the ring mode did not lie entirely within the crystal. Crystal resonators in this geometry were difficult to fabricate since it was hard to maintain the precise alignment of the crystals as they were tranferred end for end to polish the curved surfaces or on edge for the TIR surface.

We designed the crystal resonator geometry shown in Figure 8 to make fabrication easier. The new resonator geometry consists of a single curved surface that is coated and serves as the input coupler mirror plus two flat surfaces oriented to complete the resonator and serve as total internal reflecting surfaces. One leg of the ring cavity mode is parallel to the x-axis of the

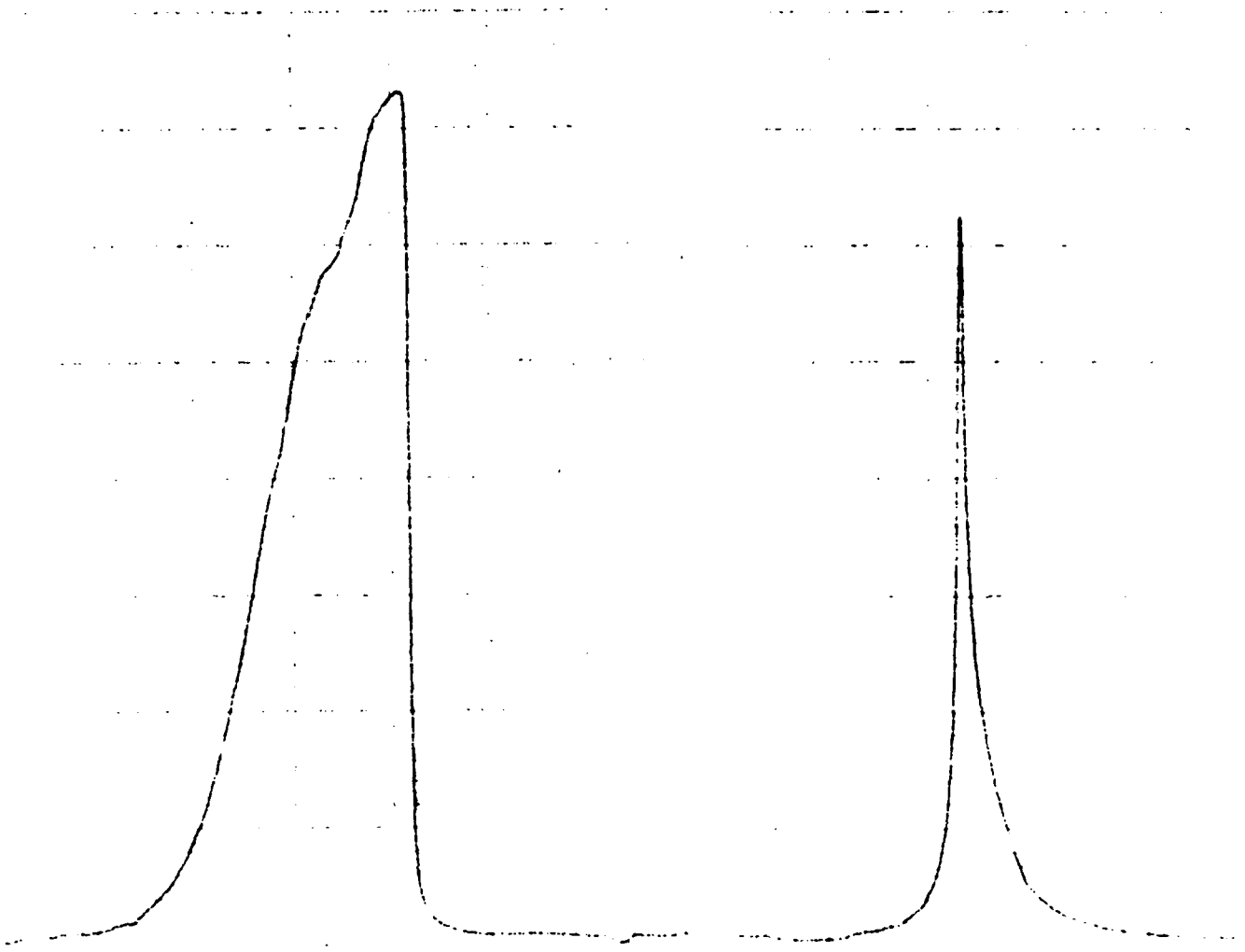

Figure 7: Assymmetry of Transmission Through a Monolithic Magnesium Oxide Resonant Doubler Crystal. The left trace shows the variation of the transmission of incident single frequency 1064nm light through the monolithic linear doubler as the 1064nm frequency is scanned in the same direction as the thermally induced frequency shift of the doubler crystal. The right trace shows the variation through the same resonance in the opposite direction. The vertical dimension is transmission. The horizontal dimension is frequency; the scale is 50 MHz per centimeter. The FWHM of the left trace is about 100 MHZ; the FWHM of the right trace is about 14 MHZ.

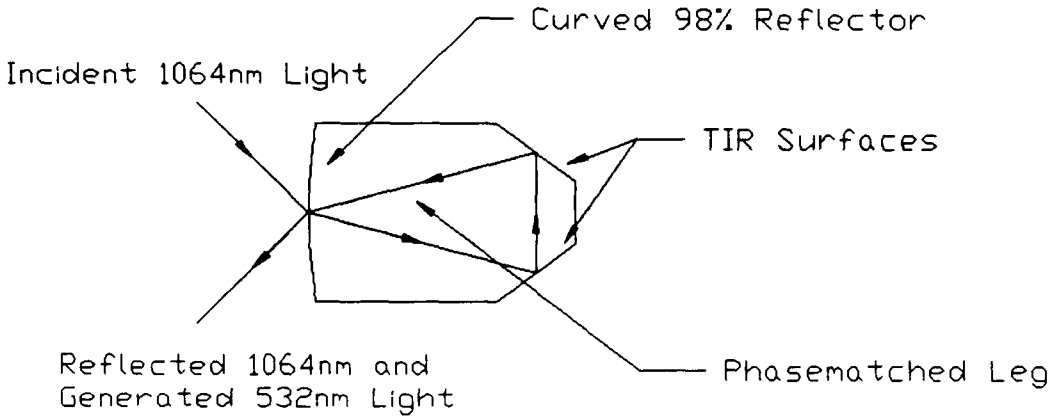

Figure 8: New Monolithic Resonant Ring Doubler Crystal. The cavity consists of one curved and coated surface plus two flat total internal reflecting surfaces. One leg of the ring mode is parallel to the x-axis of the MgO:$LiNbO_3$ crystal. The plane of the ring is perpendicular to the y-axis of the crystal. The "input mirror" coating on the curved surface is designed to "impedance match" the cavity, i.e., has transmission equal to the internal losses of the resonant cavity. The incident 1064nm light is polarized parallel to the y-axis of the crystal and the generated 532nm light is polarized parallel to the z-axis.

$MgO:LiNbO_3$. Since the orientation of the ring cavity mode is defined during the fabrication of the crystal, we designed and built tooling to precisely position and hold the crystals during the fabrication.

Crystals were X-rayed to determine the orientation of the axes and reference surfaces ground. Then the curved surfaces were ground and optically polished. We were able to fabricate up to seven crystals at a time at this step. Next, the crystals were aligned with a He-Ne laser on stainless steel crystal holders and bonded with uv cure adhesive. These parts were then attached to a base and one TIR surface on each of up to four crystals were ground and optically polished. Finally, the crystals were flipped over and the other TIR surface polished.

The advantages of the new geometry are the ability to fabricate a number of crystals simultaneously and the replacement of one curved and optically coated surface with a TIR surface. This reduces the expense of fabrication and coating and is likely to provide a lower loss high reflector. A secondary benefit is the fact that the incident 1064nm light and the reflected 1064nm and generated 532nm light are oriented 90^o relative to each other.

We obtained new $MgO:LiNbO_3$ material from Crystal Technology [11]. Our phasematching tests of this material with a pulsed laser indicated good axial uniformity and good second harmonic conversion efficiency. Also, optical quality was good.

We fabricated four crystals. Optical inspection of the fabricated parts with a He-Ne laser indicated that the ring cavity modes were contained within the crystals and were well centered. The crystals had their tops and bottoms coated with gold to serve as electrodes for electro-optic tuning and three had optical coatings applied to the curved surfaces. These coatings were specified to be $98.5\pm0.5\%$ reflectors for s-polarization at 1064nm at 45^o angle of incidence. In addition, the coating was to have as high a transmission at 532nm for p-polarization as possible.

A completed crystal is shown Figure 9. The crystal and a new version of the platinum heater-sensor element were incorporated in the assembly shown in the photograph in Figure 10.

We obtained 5 mW of cw 532nm light with 48 mW of

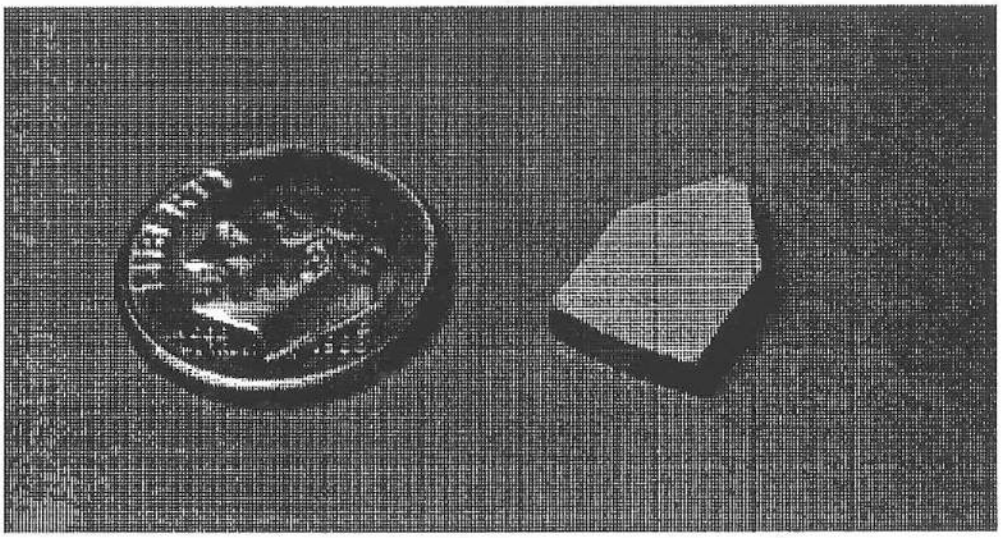

Figure 9: Resonant Ring Doubler Crystal. This magnesium oxide doped lithium niobate crystal is 12mm long by 8mm wide by 2mm thick. The optical path length for one round trip is 26mm. The curved output mirror surface has a 24mm radius of curvature and is coated as a 98.5% reflector for 1064nm light polarized as s-wave and incident at 45 degrees to the surface. The remainder of cavity is formed by two total internal reflecting surfaces. The large faces of of the crystal are y-faces and are coated with gold to act as electrodes for electro-optic tuning of the crystal.

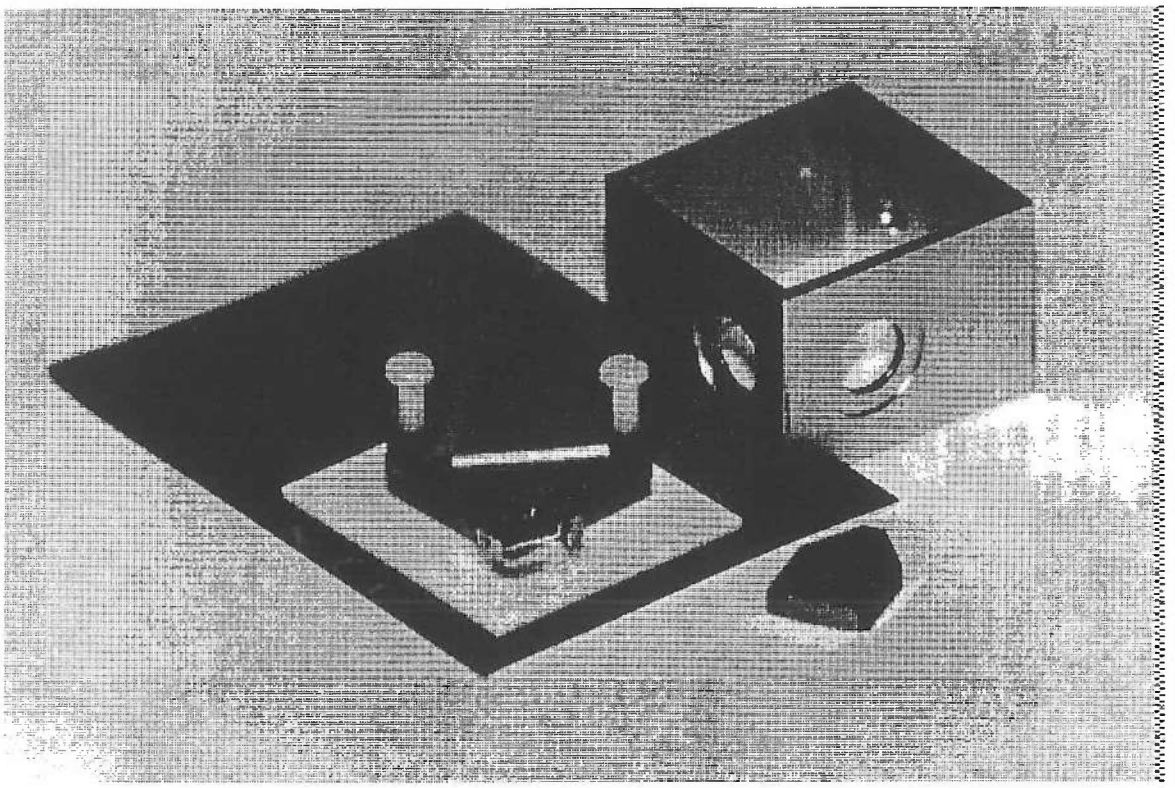

Figure 10: Photograph of the Resonant Doubler Crystal Thermal Assembly. The doubler crystal is held between two copper plates that maintain a uniform temperature around the crystal and serve as electrodes for electro-optic tuning of the crystal. The copper plates are held together with two nylon screws. The plates are mounted on top of two short sections of rectangular pyrex tubing which minimize thermal conductance to the alumina base and the outside world. The crystal is heated and held at temperature by the platinum heater and sensor element mounted on the top copper plate. The entire assembly is surrounded by an aluminum structure with holes to let the 1064nm light in and the 532nm light out. The top is another alumina plate.

1064nm light incident on the crystal and 45 mW with 200 mW incident. The 200 mW laser was optically pumped by a 500 mW diode laser so the 45 mW green output corresponds to and optical conversion efficiency from the 808nm diode laser light to the 532nm green light of 9%. Since the electrical efficiency of the diode laser was about 35%, the overall efficiency from electrical power supplied to the diode to single frequency cw 532nm light was about 3.2%.

We were able to generate 500 mW single frequency 230 ns pulses at 1064nm by modulating the diode laser current and driving the Nd:YAG laser into relaxation oscillations. An oscilloscope trace of the output of the laser is shown in Figure 11. These pulses produced 200 mW pulses at 532nm in the resonant doubler.

We measured the finesse of the ring doublers by electro-optically tuning the doubler resonant frequency with an electric field applied along the y axis of the doubler crystal. For our crystal dimensions, we needed 1440V to scan over one free spectral range, or 5.7 GHz. The measured finesse of 150 implies a total cavity loss of 4%. Since approximately 1.5% is output coupler transmission, approximately 2.5% is attributed to bulk scatter and absorption loss in the $MgO:LiNbO_3$. The second harmonic power versus fundamental data is consistent with the theory presented previously assuming g_{SH} = .001/W and intracavity loss = 2.5%.

The next experimental step was to lock the doubler into resonance with the single frequency 1064nm laser. A small 60 kHz dither voltage was applied across the doubler crystal. The 1064nm light reflected from the doubler was monitored with a photodiode. Near but not exactly on resonance, the amplitude of the reflected infrared light was modulated at 60 kHz. At resonance, the modulation was minimized. The modulation was detected with a phase sensitive amplifier tuned to the modulation frequency. The phase sensitive amplifier provided a signal to a high voltage amplifier to control the resonant frequency of the doubler and minimize the 60 kHz modulation. With this electronic control, we were able to lock the doubler in resonance with the 1064nm laser for tens of hours continuously.

Unfortunately, we observed significant degradation of the amplitude and optical quality of the generated green light over about 50 hours of continuous operation. During this time frame, the 532nm power dropped from 5 mW to less

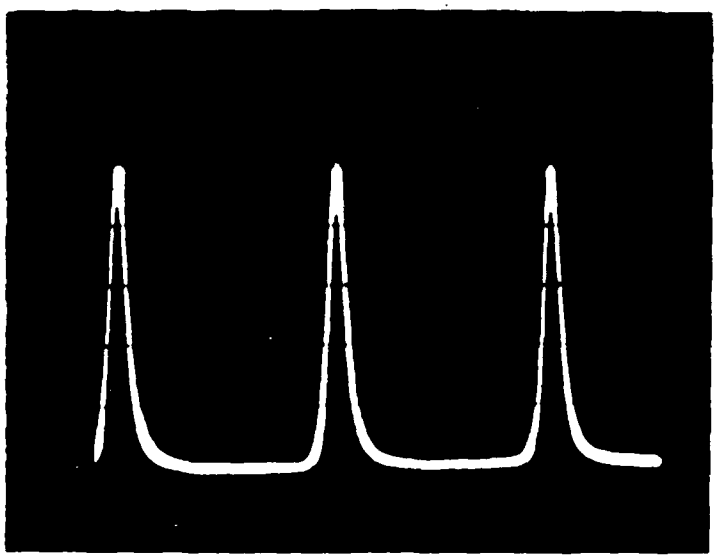

Figure 11: Relaxation Oscillations from Diode Pumped Single Frequency Non-planar Ring Nd:YAG Laser. The output consists of 500 mW peak power 230ns pulses at a 165 kHz repetition rate. These pulses produced 200 mW 532nm pulses in a magnesium oxide doped lithium niobate monolithic resonant doubler.

than 1 mW. In addition, a substantial portion of the green light was refracted from the central beam. At this time, a measurement of the cavity finesse indicated that intracavity loss had increased to about 6%.

These symptoms were consistent with photorefractive damage in the bulk of the MgO:$LiNbO_3$ introduced by the green photons. We found that cycling the doubler crystals to 170°C for several hours repaired the damage and restored the cavity finesse, beam quality and conversion efficiency to original levels. Photorefractive damage was observed in all crystals after tens of hours of operation at 532nm power levels of 5mW. Damage was apparent sooner when operating at higher green powers.

Photorefractive damage in the MgO:$LiNbO_3$ severely limits the usefulness of the material for second harmonic generation of 1064nm light. These results lead us to examine KTP and lithium diffused lithium niobate as alternate nonlinear materials.

Resonant External Doubling with KTP

KTP presents several different challenges for use in an external resonant cavity compared to lithium niobate. Both the crystal length and the effective nonlinear coefficient of KTP are smaller than for $LiNbO_3$. As a result, resonant doubling in an external cavity using KTP is even more sensitive to intracavity loss as can be seen from Figure 3. Since KTP is angle-tuned to accomplish phasematching, it is very difficult (if not practically impossible) to fabricate a monolithic doubler cavity. This stems from the fact that the location of the resonant mode of the cavity is defined by the fabrication process, eliminating the option to tune the phasematching later by tilting the crystal. Finally, since phasematching in KTP requires both an ordinary and an extra-ordinary component, some form of compensation for the o-wave and e-wave phase shift must be included in the cavity to reduce loss.

Our KTP experiments used the optical cavity shown in the photograph in Figure 12. The cavity consists of three flat high reflector mirrors and one flat 98% reflecting mirror, all coated for s-polarization, 1064nm and 45° angle of incidence. One of the high reflectors is mounted on a piezo-electric element to control the resonant frequency of the cavity. One long leg of the cavity contains an anti-reflection coated lens to image the

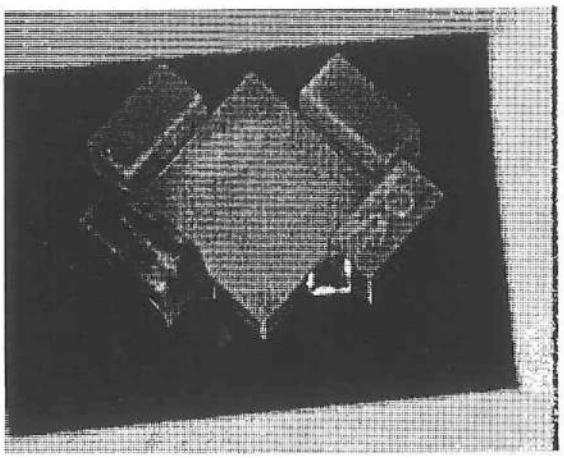

Top View

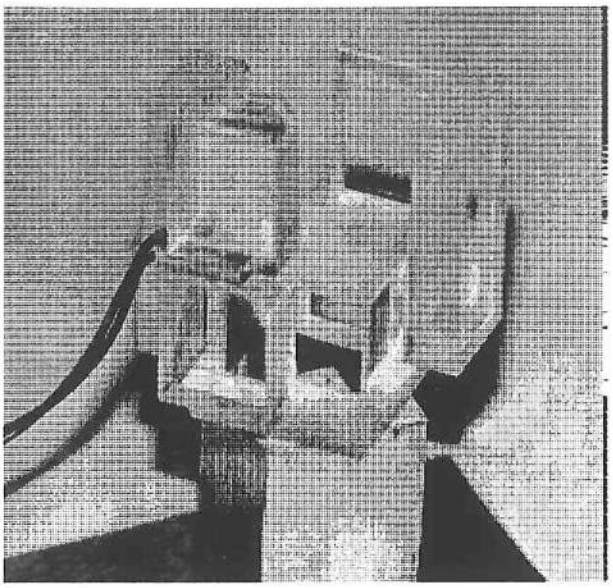

Oblique View

Figure 12: Optical Cavity for Resonant Doubling Experiments with KTP. The top view shows the four flat mirrors bonded to a quartz block. One of the mirrors is mounted on a piezo-electric transducer to permit scanning and control of the resonant frequency of the cavity. Three of the mirrors are high reflectors for 1064nm light at 45° angle of incidence. The fourth mirror is coated for 98% reflectivity.

1064nm light into the KTP crystal and form a stable optical cavity. The KTP crystal is held in the opposite leg on a rotation stage to allow angular adjustment of the crystal for phasematching.

Finesse measurements of the cavity containing only the AR coated 25mm focal length lens indicated that total intracavity loss exclusive of the output coupling was about 0.4%. Additional loss introduced by the KTP crystal oriented with the z-axis parallel to the polarization of the 1064nm light was about 0.5%. To phasematch, the crystal was rotated 45^{o} about the cavity mode axis and then tilted to maximize 532nm signal.

A total of 1mW of cw 532nm light was generated using this configuration for 100 mW of 1064nm light incident on the cavity. Conversion efficiency was limited because focussing was not optimized for the 5mm crystal length, because the o-wave and e-wave phase shift in the crystal limited the amount of 1064nm circulating power and because the output coupling was not optimized to "impedance match" the cavity. We observed that introduction of a quarter wave plate into the cavity improved second harmonic conversion efficiency by a factor of about two when oriented to compensate for the KTP phase shift. Unfortunately, the additional intracavity loss of the waveplate limited the total 532nm power to 1 mW.

We also explored other ways to compensate for the depolarization of the 1064nm light by the KTP crystal. Since KTP is electro-optic [14], we fine tuned the crystal by applying a z-axis electric field. Although we were able to cancel the depolarizing effect of the KTP with 1500 volts applied across the 3mm thick crystal, we found that the high field introduced an optical defect in the bulk of the crystal. Three crystals displayed the same phenomena. The optical defects slowly disappeared over the course of about 12 hours at 25^{o}C. Measurement of the resistance of one crystal indicated that the bulk resistivity was about 3 megaohm-cm, which is two orders of magnitude smaller than published values [15]. It is possible to obtain specially selected KTP crystals with high resistivity which do not display the electric field induced optical defects from Airtron, but these crystals are not presently available as commercial products in quantity.

We were also able to compensate for the depolarizing properties of the crystal by controlling its temperature. We found that a full wave of phase shift for the 5mm long

crystal could be introduced by varying the temperature 60°C.

Lithium Diffused Lithium Niobate Studies

A significant portion of this research program was also spent exploring the feasibility of nonlinear optical conversion using lithium diffused lithium niobate. The process of transport of lithium into congruent lithium niobate fibers to improve homogeneity, modify the ratio of lithium to niobium and thus change the phasematching temperature for second harmonic generation was studied by Y.S. Luh and co-workers at Stanford University [16]. They found that soaking congruent lithium niobate crystals in Li_2O vapor liberated from a mixture of lithium carbonate and niobium pentoxide powders could produce satisfactory crystals.

Luh et al [16] observed complete equilibration of lithium diffusion in 0.7mm thick crystals after 67 hours of processing at 1100°C. They observed a shift in the phasematching temperature for second harmonic generation of 1064nm light from 4°C to 238°C. This elevated phasematching temperature is above the temperature required for annealing photorefractive damage which was the major problem with $MgO:LiNbO_3$.

Since it was more convenient to fabricate our resonant doublers using thicker crystals, we studied lithium diffusion in these thicker parts. Our initial experiments were with 1mm thick crystals. We were able to produce diffused crystals with satisfactory phasematching characteristics after about 150 hours of processing.

Our experiments with 2mm thick crystals were less successful. 2mm thick crystals that were processed for 200 hours continuously ended up shattered along the entire length and had nonuniform multi-color discoloration. We attributed the problem to stresses introduced due to incomplete lithium diffusion and thermal cycling from room temperature, up to 1100°C and back to room temperature. The next crystals were held at processing temperature for 500 hours continuously (three weeks!). These crystals survived the processing, did not shatter and had no sign of the discoloration observed in crystals which were processed for only 200 hours. Phasematching curves for several positions in one crystal are shown in Figure 13. These curves indicate good axial homogeneity. Visual

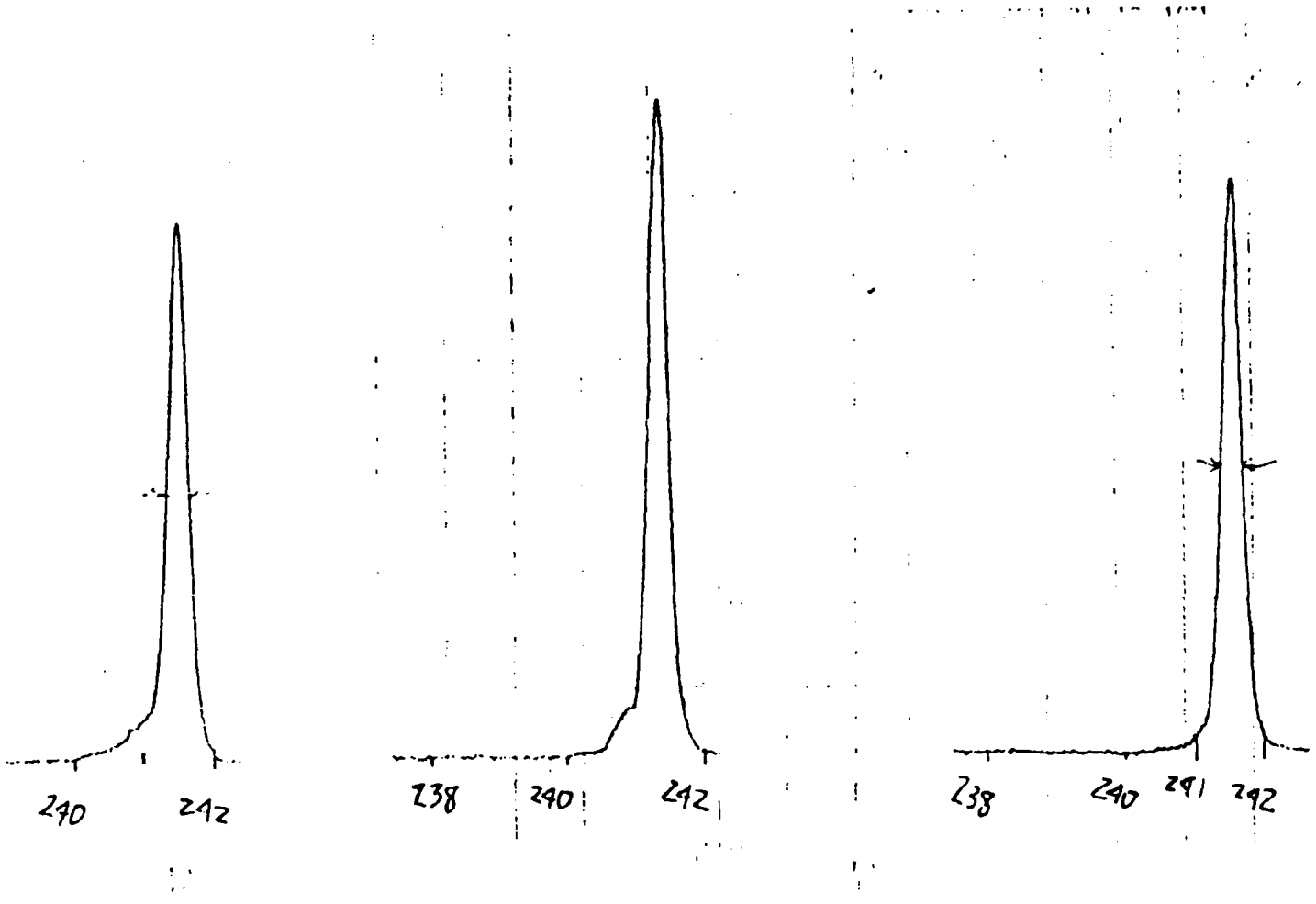

Figure 13: Phasematching Curves for 1064nm Light in Lithium Diffused Lithium Niobate. The curves are for the top (left trace), middle (center trace) and bottom (right trace) of a 2mm thick 30mm long lithium niobate crystal that was diffused for 500 hours at 1100 degrees Centigrade. The phasematching temperature for all three locations is 241.5 degrees C. Full width at half maximum is about 0.3 degrees, indicating that the phasematchable length of the crystal is essentially the entire 30mm.

inspection however revealed that transverse gradients existed in the crystals. Subsequent processing for up to 2000 hours was inadequate to remove the transverse gradients. These optical flaws lead to significant scattering of the generated second harmonic beam and represent optical losses that would be unacceptable in a high Q resonant cavity. In discussions with Dr. Martin Fejer of Stanford University and Dr. Peter Bordui of Crystal Technology, we determined that the inhomogeneities may be other phases of lithium niobate, i.e. Li_3NbO_4 as well as the desired $LiNbO_3$. It should be possible to avoid these problems with proper processing of the crystals and further research is necessary.

To test the compatibility of optical coatings on lithium niobate at temperatures near phasematching, samples of lithium niobate were coated with high reflector coatings consisting of alternating quarter wave layers of HfO_2 and SiO_2 centered at 1064nm. Both x-plates and z-plates were coated. Coated parts were then thermally cycled to test for crazing of the coatings. Parts were ramped up to the test temperature in two hours, held at temperature for two hours and brought back to 25°C in two hours. We found that the coatings did not fail at 100°C or 150°C, but were unable to withstand a thermal cycle to 200°C. These results indicate that some other coating design would be necessary for monolithic diffused lithium niobate resonant doublers. (So-called "soft coatings" are not expected to handle the 200°C thermal cycle either.)

PULSED LASER FREQUENCY DOUBLING EXPERIMENTS

Efficient second harmonic conversion is easier with higher power lasers such as Q-switched solid state lasers. We measured the second harmonic conversion efficiency in $MgO:LiNbO_3$, KTP and lithium diffused lithium niobate using LIGHTWAVE Electronics Model 110 diode pumped Q-switched lasers. These lasers can produce 50 uJ 5ns pulses at several kHz repetition frequencies. Pulse energies of 50 uJ in 5ns correspond to 10 kW of peak power. The output beam is TEM_{00}. The experimental arrangement for these measurements consists of the 110 laser, a lens to focus the laser into the nonlinear crystal, filters and a power meter.

In these experiments, the output of the 110 laser was confocally focussed into the crystal and the repetition frequency of the laser was adjusted to maximize the <u>average</u> power at the second harmonic. Some sacrifice in conversion efficiency is made because peak power (and hence peak second harmonic conversion efficiency) occurs for laser repetition rates less than about 1 kHz. At higher rep rates, the output pulse energy of the 110 decreases and the pulse duration increases, leading to lower peak power. Consequently, conversion efficiency is reduced. <u>Average</u> power at the fundamental, however, continues to increase as the rep rate increases. As a result, the rep rate for maximum average power at the second harmonic does not necessarily correspond to the rep rate for the maximum conversion efficiency.

Our results are summarized in Table I. We measured over 50% energy conversion from 1064nm to 532nm using a 25mm long lithium diffused lithium niobate crystal. The crystal was temperature phasematched for 1064nm at 238°C. We obtained over 44% conversion with a 15mm $MgO:LiNbO_3$ crystal (temperature phasematched at 115°C) and about 34% with an angle phasematched 5mm KTP crystal. The higher conversion efficiencies with lithium niobate crystals are almost certainly due to the longer crystal lengths. Longer KTP crystals are not readily commercially available at this time.

We also investigated the generation of the fourth harmonic of 1064nm at 266nm using our Model 110 diode pumped Q-switched laser. The experimental apparatus is shown in Figure 14. For these experiments, the second harmonic at 532nm was generated in angle tuned KTP. The average power at 532nm was 32.5 mW for 95 mW of average

TABLE I

SECOND HARMONIC CONVERSION EFFICIENCY

CRYSTAL	LENGTH (mm)	ENERGY CONVERSION EFFICIENCY
KTP	5	34.2%
MgO:$LiNbO_3$	15	44.2%
Diffused $LiNbO_3$	25	50.3%

TABLE II

FOURTH HARMONIC GENERATION EXPERIMENTAL RESULTS

WAVELENGTH (nm)	AVERAGE POWER (mW)	PULSE ENERGY (uJ)	PEAK POWER (kW)
1064	95	23.8	2.2
532	32.5	8.1	1.1
266	5.1	1.3	0.24

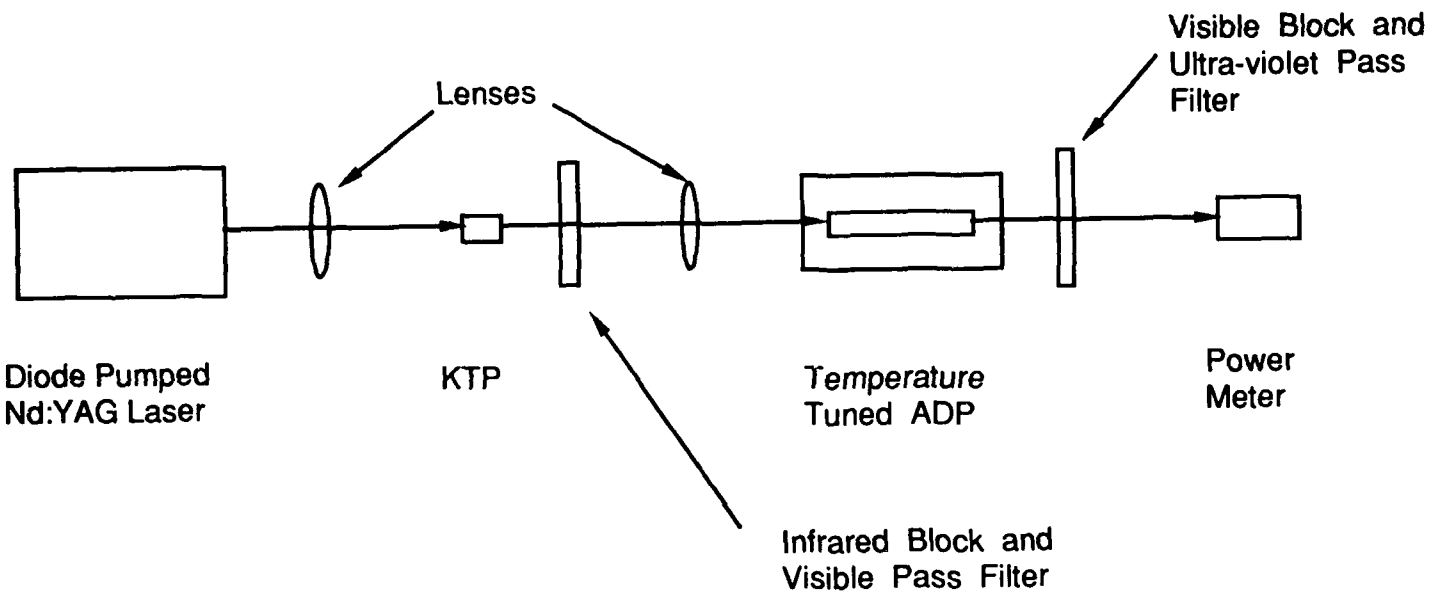

Figure 14: Experimental Apparatus for Generation of the 266nm Fourth Harmonic of a Diode Pumped Q-switched Nd:YAG Laser. The 532nm second harmonic is generated in angle tuned KTP. The residual fundamental is filtered by an infrared block/visible pass KG-3 filter which passes 78% of the 532nm light. The fourth harmonic is generated by frequency doubling the 532nm light in temperature tuned ADP. Phasematching temperature was 50 degrees Centigrade. Five milliwatts of average power at 266nm was generated for 95 mW of average power (2.2 kW peak power pulses) at 1064nm.

power at 1064nm incident on the KTP. The residual 1064nm light was filtered from the beam with a KG-3 filter which transmitted 78% of the 532nm light. Thus, about 25 mW of green light was available for subsequent doubling to 266nm. The fourth harmonic at 266nm was generated in a 50mm long temperature tuned ammonium dihydrogen phosphate (ADP) crystal. The kilowatt peak power and good beam quality at 532nm provided for 20% energy conversion to the fourth harmonic at 266nm. Phasematching temperature was 50°C in the ADP. Over 5 mW of average ultraviolet power with peak power of 240 Watts was generated from the diode pumped all solid state system. The experimental conditions for our fourth harmonic measurements are summarized in Table II.

CONCLUSIONS AND RECOMMENDATIONS

In this research program we began the initial development of diode pumped single frequency cw lasers and diode pumped Q-switched lasers. We studied techniques to efficiently convert the infrared outputs of these lasers to the visible spectral region. We generated 45 mW of cw single frequency 532nm light with 25% conversion efficiency in an external monolithic magnesium oxide doped lithium niobate doubling crystal. The efficiency of conversion from diode laser light to cw single frequency green light was 9% and overall efficiency from electrical power to the diode laser to the green was over 3%. This device produced over 200 mW green pulses when pumped with 500 mW single frequency 1064nm pulses. The doubler crystal was frequency locked to the 1064nm laser for tens of hours using electro-optic control of the doubler crystal resonant frequency. Bulk absorption and scatter losses in the crystal prevented greater conversion efficiencies. Photorefractive damage in the $MgO:LiNbO_3$ lead to severe degradation in the conversion efficiency over the course of tens of hours and limits the usefulness of this material.

We generated mW levels of 532nm light using KTP in an external cavity. We identified voltage induced optical damage in KTP as a problem in these experiments. Optimization of cavity design, selection of KTP crystals which have lower ionic conductivity and the use of higher power single frequency lasers such as nonplanar ring lasers pumped by higher power diodes or lamp pumped lasers which are frequency locked to single frequency sources may improve the viability of this approach.

Our experiments verified that lithium diffusion in lithium niobate crystals shifts the phasematching temperature for 1064nm light to about 238^{o}C. Unfortunately, we were unable to produce satisfactory crystals in sizes that we felt could be reliably fabricated. We also found that high reflector coatings centered at 1064nm on lithium niobate fail at about 200^{o}C.

Energy conversion efficiencies as high as 50% were observed using LIGHTWAVE Electronics Model 110 diode pumped Q-switched lasers and diffused lithium niobate crystals. We also observed 34% conversion efficiencies using KTP. Finally, we were able to produce 5 mW of average power at 266nm with a diode pumped all solid state system.

Our results from this research program indicate that efficient sources of visible laser light can be produced using nonlinear optical techniques. For small cw visible sources, resonant doubling of the single frequency lasers is a preferred approach. The laser can exceed 50% optical to optical conversion efficiency and the stable frequency provides for fairly simple electronics to lock the doubler cavity to the laser. The major difficulty at this point is the doubling material. MgO:$LiNbO_3$ suffers from photorefractive damage which effectively limits lifetime to tens of milliwatt-hours of operation. Other potential materials are lithium-diffused lithium niobate, periodically poled lithium niobate, potassium niobate, barium sodium niobate, and KTP. The last three are known to not suffer from photorefractive damage. Diffused lithium niobate phasematches above the temperature required to anneal damage. KTP will become more viable as single frequency laser powers approach one watt.

The conversion efficiency for diode pumped Q-switched lasers is already respectable. Higher average powers await the arrival of even more powerful diode laser sources.

REFERENCES

[1] Robert L. Byer, "Diode laser-pumped solid state lasers," Science, Vol. 239, pp. 742-747, Feb. 12, 1988.

[2] Tso Yee Fan and Robert L. Byer, "Diode laser-pumped solid-state lasers," IEEE J. Quantum Electron., Vol. 24, pp. 895-912, June, 1988.

[3] W. Streiffer, D.R. Scifres, G.L. Harnagel, D.F. Welch, J. Berger, and M. Sakamoto, "Advances in diode laser pumps," IEEE J. Quantum Electron., Vol. 24, pp. 883-894, June, 1988.

[4] Thomas J. Kane and Robert L. Byer, "Monolithic, unidirectional single-mode Nd:YAG ring laser," Optics Lett., Vol. 10, pp. 65-67, January, 1985.

[5] A. Ashkin, G.D. Boyd, and J.M. Dziedzic, "Resonant optical second harmonic generation and mixing," IEEE J. Quantum Electron., Vol. QE-2, pp. 109-124, June, 1966.

[6] William J. Kozlovsky, C.D. Nabors, and Robert L. Byer, "Efficient second harmonic generation of a diode-laser-pumped cw Nd:YAG laser using monolithic MgO:$LiNbO_3$ external resonant cavities," IEEE J. Quantum Electron., Vol. 24, pp. 913-919, June, 1988.

[7] Walter Koechner, Solid-State Laser Engineering, Second edition, Springer-Verlag, Berlin, 1988, p. 480.

[8] Frits Zernike and John E. Midwinter, Applied Nonlinear Optics, Wiley, New York, 1973, pp. 112-120.

[9] T. Baer, "Large-amplitude fluctuations due to longitudinal mode coupling in diode-pumped intracavity-doubled Nd:YAG lasers," J. Optical Soc. Am.B, Vol. 3, pp. 1175-1180, September, 1986.

[10] Michio Oka and Shigeo Kubota, "Stable intracavity doubling of orthogonal linearly polarized modes in diode-pumped Nd:YAG lasers," Optics Lett., Vol. 13, pp. 805-807, October, 1988.

[11] J.L. Nightingale, W.J. Silva, G.E. Reade, W.J. Kozlovsky and R.L. Byer, "Second harmonic generation in MgO doped lithium niobate," Proc. SPIE, Vol. 681, SPIE, Bellingham, Wa.,1987, pp. 20-26.

[12] D.A. Bryan, R.R. Rice, Robert Gerson, H.E. Tomaschke, K.L. Sweeney and L.E. Halliburton, "Magnesium-doped lithium niobate for higher optical power applications," Opt. Engineering, Vol. 24, pp. 138-143, Jan.-Feb., 1985.

[13] R.F. Belt, G. Gasherov and Y.S. Liu, "KTP as a harmonic generator for Nd:YAG lasers," Laser Focus, Vol. 21, pp. 110-112, October, 1985.

[14] J.D. Bierlein and C.B. Arweiler, "Electro-optic and dielectric properties of $KTiOPO_4$," Appl. Phys. Lett., Vol. 49, pp. 916-919, 1986.

[15] J.D. Bierlein, A. Ferretti, and M.G. Roelofs, "$KTiOPO_4$ (KTP) : A new material for optical waveguide applications," SPIE-Boston, Paper 994-22.

[16] Y.S. Luh, M.M. Fejer, R.L. Byer, and R.S. Feigelson, "Stoichiometric LiNbO3 single-crystal fibers for nonlinear optical applications," J. Crystal Growth, Vol. 85, p. 264, 1987.